

Effects of perpendicular interlayer coupling strength on canting angles of TbCo-sublattice magnetization

Meng-Shian Lin,¹ Hao-Cheng Hou,¹ Yun-Chung Wu,¹ Po-Hsiang Huang,¹ Chih-Huang Lai,^{1,*} Hsiu-Hau Lin,^{2,3,†} Hong-Ji Lin,⁴ and Fan-Hsiu Chang⁴

¹Department of Materials Science and Engineering, National Tsing Hua University, Hsinchu 30013, Taiwan

²Department of Physics, National Tsing Hua University, Hsinchu 30013, Taiwan

³Physics Division, National Center for Theoretical Sciences, Hsinchu 30013, Taiwan

⁴National Synchrotron Radiation Research Center, Hsinchu 300, Taiwan

(Received 16 October 2008; published 30 April 2009)

We investigate the perpendicular interlayer coupling between Co/Pt multilayers and Co/TbCo bilayers through the Ru spacer with various thickness. The canting angles of the Tb and Co moments are determined by x-ray magnetic circular dichroism. We observe that the interlayer exchange coupling oscillates and aligns Co and Tb moments in *opposite* directions. As a consequence, the canting angles of the Tb and Co moments correlate with the strength of the interlayer coupling and agree with our theoretical calculations as well. The opposite alignment on the TbCo-sublattice magnetizations from the interlayer coupling cannot be viewed as an effective magnetic field and thus is unique with potential applications for spintronics devices.

DOI: 10.1103/PhysRevB.79.140412

PACS number(s): 75.30.Et, 75.25.+z, 75.50.Gg, 75.70.Cn

Carrier-mediated exchange coupling plays a crucial role in itinerant magnetism for its fundamental importance and promising potentials for applications.¹⁻⁴ Early investigations of the oscillatory interlayer exchange couplings mainly focus on the transition-metal and rare-earth magnetic multilayers with in-plane anisotropy.^{1,2} However, from the practical perspective, it is desirable to design multilayers (MLs) with perpendicular anisotropy that helps shrink the magnetoresistive random access memory (MRAM) cells.⁵ Possible candidates include Co/Pt multilayers, TbCo, and FePt, where the perpendicular interlayer coupling between Co/Pt MLs and Co/TbCo bilayers through Ru spacer has been reported.⁶ Note that the simultaneous presence of two kinds of magnetic moments in TbCo thin film^{7,8} complicates the story and these systems are not yet fully understood in the literature.

The interlayer exchange coupling mediated by the itinerant carriers is similar to the Ruderman-Kittel-Kasuya-Yosida (RKKY) between impurity spins.⁹⁻¹¹ Though the RKKY-type models capture the correct oscillatory period, their estimates on the coupling strength are less reliable since they do not adequately describes magnetism in transition metals. The itinerancy of electrons/holes, the quantum confinement inside the narrow spacer, and the interface reflections are all crucial in determining the strength of the interlayer coupling.⁹⁻¹¹ In addition, competitions between the carrier-mediated interactions and other short-ranged magnetic coupling often bring out rich and interesting phenomena.¹²⁻¹⁴ For instance, in [Co/Pt]/Ru MLs with perpendicular anisotropy, the coexistence of antiferromagnetic (AF) and ferromagnetic (F) domains were observed by tuning the layer thickness or by applying the magnetic field.¹² The simultaneous presence of the perpendicular orange peel interactions and the oscillatory RKKY ones leads to the net coupling in [Co/Pt]-based spin valves.¹³ Furthermore, studies on the Co/Cu/[Fe/Ni]/Cu(100) multilayers reveal that the interlayer coupling between the Co and Fe films serves as an effective magnetic field to align the magnetic stripes of the Fe/Ni film.¹⁴ It is interesting that the evolution of the stripe-domain

width only depends on the strength of the interlayer coupling but not sensitive to its sign. In addition, the variations of magnetic configuration generated by the coupling between TbFe and Co/Pt have been studied by using x-ray magnetic circular dichroism (XMCD).¹⁵ The altered XMCD intensity was attributed to the existence of domain wall and/or lateral domain formations.

Motivated by the rich physics and the open questions in these magnetic structures, we investigate the effects of the interlayer coupling between Co/Pt MLs and Co/TbCo bilayers through a thin Ru spacer. Note that the alloys composed of heavy rare earth (such as Tb) and transition metal (such as Co) are ferrimagnetic.¹⁶ The intrinsic magnetic anisotropy in TbCo thin films aligns the Tb and Co moments antiferromagnetically, but it is not strong enough to hold the Tb and Co magnetizations strictly antiparallel.^{7,8} The interlayer coupling, sensitively depending on the spacer thickness, may compete with the intrinsic magnetic interactions in TbCo films, leading to the change in the canting angles. Ignoring the biquadratic coupling momentarily, one may naively expect that the interlayer coupling acts as an effective magnetic field that tends to align both Tb and Co moments along the same direction. If so, theoretical calculations show that the relative angle ϕ_r between Tb and Co moments remain more or less constant since both canting angles increase/decrease at the same time.

It is surprising that we found the opposite: ϕ_r oscillates and correlates with the strength of the interlayer coupling as the spacer thickness varies. We are able to measure the canting angles ϕ_{Tb} and ϕ_{Co} separately by x-ray magnetic circular dichroism (XMCD). As the spacer thickness changes, they oscillate out of phase, implying that the interlayer coupling aligns Tb and Co moments in *opposite* directions. As a result, when the strength of the interlayer coupling is large, the relative angle ϕ_r is pulled larger as well. On the other hand, ϕ_r comes back to its natural value when the coupling strength is small. Our experimental observation reveals the interlayer coupling with opposite signs in the magnetic thin

film composed of two-sublattice magnetizations through canting-angle measurements.

In the following, we start with the experimental details and explain how we arrive at the above claims. The samples of Si/Ta(3)/Pt(7)/[Co(0.5)/Pt(2)]₅/Co(0.5)/Ru(*t*_{Ru})/Co(0.5)/Tb_{25.5}Co_{74.5}(17)/Pt(2) (unit: nm) were prepared by using UHV sputtering at room temperature. The TbCo layers were cosputtered using Tb and Co targets. The substrates were rotated on the top of targets with a revolution speed of 15 rpm during the deposition of TbCo layers. We use transmission electron microscopy (TEM) to examine the microstructure of the films. The cross-sectional TEM images (not shown) of the sample reveal a clear layered structure of Co/Pt MLs and an amorphous TbCo layer. The magnetic properties of the films were measured using a vibration sample magnetometer and polar magneto-optical Kerr effect. In our Co/TbCo bilayers, the magnitude of Co moment was larger than that of Tb moment so that the direction of Co moment dominates the net magnetization in the film.¹⁷

The canting angles of the Tb and Co magnetizations were measured by XMCD, possessing sharp element-specific sensitivity,^{18,19} at the Dragon beamline 11A at the National Synchrotron Radiation Research Center in Taiwan. The XMCD spectra measured at remnant state after saturation with the circular-polarized light were obtained in a total electron yield mode on the Tb *M*_{4,5} edge and Co *L*_{2,3} edge with probing depth about 5 nm. The surface-sensitive XMCD technique thus enables us to probe the top TbCo layer only. The polarized x rays were incident on the samples at angles $\pm\theta_0 = \pm 30^\circ$ denoting *P* and *A* incidences schematically shown in Fig. 1. The canting angle of the moment can be deduced from the formula,^{20,21}

$$\tan \phi = \cot \theta_0 \left(\frac{I_P - I_A}{I_P + I_A} \right), \quad (1)$$

where *I_P* and *I_A* are XMCD intensities for the *P* and *A* incidences. If the moment is perpendicular to the film surface, the canting angle ϕ is either at 0 or 180°. In this case, XMCD intensities for the Tb *M*₅ edge (or Co *L*₃ edge) with the *P* and *A* incidences should be identical. Our XMCD spectra in Fig. 1 show a negative peak at Tb *M*₅ edge and a positive peak at Co *L*₃ edge, confirming that the Tb and Co moments are nearly antiparallel.

However, as shown in Fig. 1, we observed significant intensity difference of XMCD spectra for Tb *M*₅ edge and Co *L*₃ edge between *P* and *A* incidences, revealing that the Tb and Co moments are indeed not aligned along the normal direction of the film but tilted with canting angles ϕ_{Tb} and ϕ_{Co} , respectively. Varying the Ru thickness, the measured canting angles ϕ_{Tb} and ϕ_{Co} are shown in Fig. 2. It is clear that their variations are out of phase. To further clarify the effects of interlayer coupling on the canting angles, we investigated a single TbCo layer alone, deposited at the same condition as the [Co/Pt]₅/Co/Ru/Co/TbCo samples. The canting angles of Tb and Co moments for the single TbCo layer (without Co/Pt MLs) are $\phi_{\text{Tb}} \sim 167^\circ$ and $\phi_{\text{Co}} \sim 7^\circ$. On the other hand, we also measured the canting angle of Co in Co/Pt MLs and no canting angle was found because Co/Pt MLs possess strong perpendicular anisotropy. In addition,

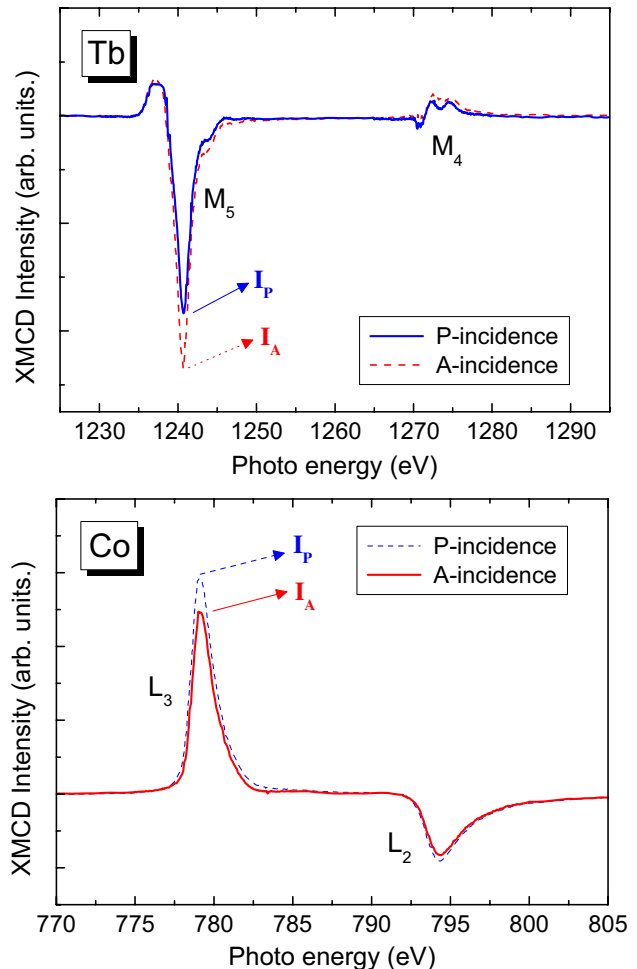
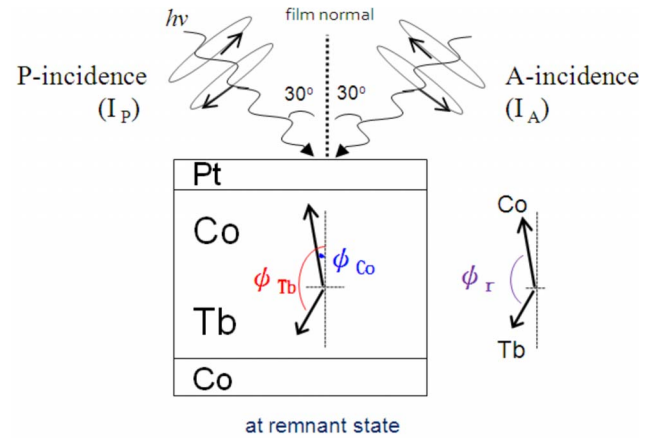


FIG. 1. (Color online) XMCD spectra of Tb *M*_{4,5}-edge and Co *L*_{2,3}-edge with *P* and *A* incidences on the [Co/Pt]₅/Co/Ru(*t*_{Ru})/Co/TbCo samples with the spacer thickness *t*_{Ru}=1.25 nm. The experimental setup is shown schematically here with the definitions for the canting angles.

our measurements were taken at the remnant state after saturation without domain structure in magnetic force microscopy (MFM) images (not shown). Thus, we can exclude the possibility that the XMCD intensity was altered by the different domain configurations as reported in Ref. 15.

In principle, the canting angles of Co and Tb may have

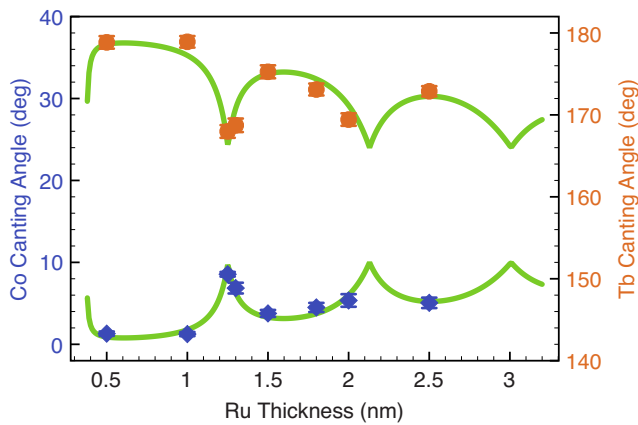


FIG. 2. (Color online) The canting angles of the Co (blue diamonds) and the Tb (orange dots) moments in TbCo layer at different spacer thickness. The solid lines are the numerical solutions for the canting angles from the theoretical model discussed.

distributions in the amorphous TbCo thin film. The TbCo alloys were reported to possess noncollinear structures, and the mean opening angle of the cone formed by the Tb moments can also be determined by using the XMCD spectra in which the projected Tb moments along the film normal direction are measured.²² The Tb moments were assumed to be randomly distributed around the anisotropy axis (film normal direction), and the mean opening angle was deduced from the ratio of the projected moment to that of the theoretical bulk value of Tb. However, this opening angle of the cone structure is different from our measured canting angle, which is defined as the angle between the film normal and the average anisotropy axis of Tb or Co [vector sum of Tb (or Co) moment]. The XMCD measurements give the average directions of the magnetic moments from the distribution. The codeposition scheme with substrates rotating on the top of sputtering guns gives rise to a preferential azimuthal direction for both canting angles. Then, we found that the canting angles are along the tangential direction of the rotating paths.^{23,24} The coplanar behavior makes the relative angle between the Tb and Co moments rather straightforward, $\phi_r = \phi_{\text{Tb}} - \phi_{\text{Co}}$, without further geometric complications.

Now we turn to the measurements for interlayer coupling J via hysteresis loops shown in Fig. 3. They demonstrate the perpendicular magnetizations of Co/Pt MLs and Co/TbCo bilayers with clear antiferromagnetic and ferromagnetic couplings at $t_{\text{Ru}}=1$ and 2 nm from how the minor loops are shifted accordingly. Gathering loop shifts at different spacer thickness, the oscillatory nature of the interlayer coupling is revealed, as shown in Fig. 4. Note that we plot the strength of the coupling since the relative angle ϕ_r does not depend on whether the overall coupling is ferromagnetic or antiferromagnetic. For comparison, the relative angle ϕ_r is also plotted in Fig. 4, which clearly correlates with the strength of the interlayer coupling. Note that when J approaches zero at $t_{\text{Ru}}=1.25$ nm, the relative angle is $\phi_r=159^\circ$, close to that observed in the single TbCo film ($\phi_r \approx 160^\circ$) without Co/Pt MLs. Furthermore, since the measured ϕ_{Tb} and ϕ_{Co} for the single-layer TbCo sample are close to those in the [Co/Pt]₅/Co/Ru/Co/TbCo samples with $J \approx 0$, it shows that

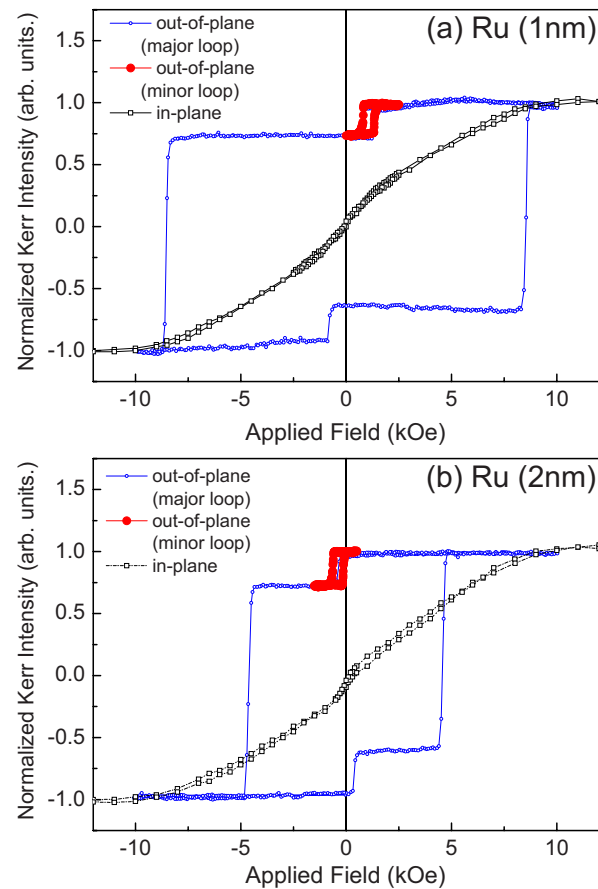


FIG. 3. (Color online) Hysteresis loops of the [Co/Pt]₅/Co/Ru(t_{Ru})/Co/TbCo samples with (a) $t_{\text{Ru}}=1$ nm and (b) $t_{\text{Ru}}=2$ nm.

the biquadratic interlayer coupling is not of crucial importance.

We developed a simple model to explain the correlation between ϕ_r and $|J|$. First of all, theoretical models for differ-

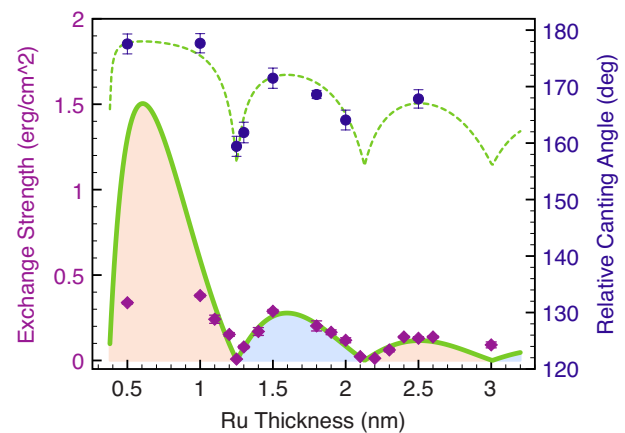


FIG. 4. (Color online) The strength of interlayer coupling $|J|$ (purple diamonds) and the relative angle (blue dots) versus the thickness of the Ru spacer in [Co/Pt]₅/Co/Ru/Co/TbCo samples. The pink and blue shaded colors denote the AF and the F regimes of the overall interlayer coupling. The solid and dashed lines are theoretical fits to the experimental data.

ent microscopic mechanisms^{9,10} all predict the same functional form of the interlayer coupling,

$$J(x) = \frac{A}{x^2} \sin(Qx + \delta), \quad (2)$$

where the oscillatory wave number $Q \approx 3.58 \text{ nm}^{-1}$ and the phase shift $\delta \approx 1.8$ can be determined from the nodes where the interlayer coupling is almost zero. With one parameter $A \approx 0.75$, we can then fit all data in Fig. 4. The pinning energy for the system is $E(\phi_i) = E_c(\phi_i) - \sum_i \alpha_i J(x) \phi_i$, where $i = \text{Co}$ and Tb and α_i denotes the relative strength of the interlayer coupling to the different magnetic moments. Making use of the Taylor expansion when minimizing the energy $\partial E / \partial \phi_i = 0$, the canting angles can be determined,

$$(\phi_i - \phi_i^*) + \gamma_i J(x) \sin \phi_i = 0, \quad (3)$$

where $\gamma_i = \alpha_i / (\partial^2 E_c^* / \partial \phi_i^2)$ are the only fitting parameters. The natural canting angles ϕ_i^* are determined at the nodes of the interlayer coupling. With the choice of $\gamma_{\text{Co}} = 450 \times (\pi/180)$ and $\gamma_{\text{Tb}} = -400 \times (\pi/180)$, the numerical solutions agree quantitatively with the experimental data shown in Fig. 2. It is important to emphasize that the couplings γ_i are different in signs, meaning the interlayer coupling tends to align Co and Tb moments in *opposite* directions. That is why their canting angles oscillate out of phase as the spacer thickness

changes. Due to the coplanar structure, the relative angle can be extracted easily and is compared with the strength of the interlayer coupling as shown in Fig. 4.

The simultaneous presence of the intrinsic magnetic anisotropy and the interlayer couplings with opposite signs in the TbCo thin film makes the system rather different. Since the Tb and Co moments are canted in nearly opposite directions, the net moment can be small. However, both moments are coupled to the itinerant carriers and can produce significant spin torque or influence the spin-dependence transport through the magnetic multilayers, despite the overall net moment is small. Thus, the magnetic junction with the TbCo layer offers a window for manipulating spin configurations and also the transport properties coupled to the canted moments. The quantitative agreement between the experiment and the theory for the TbCo-sublattice magnetization shows that the effects of the carrier-mediated coupling on the canting angles are under control and thus desirable for potential applications.

The authors are grateful for the financial support from the National Science Council of Republic of China under Grants No. NSC95-2112-M-007-054-MY3 (C.H.L.), No. NSC97-2622-E-007-002 (C.H.L.), No. NSC-96-2112-M-007-004 (H.H.L.), and No. NSC-97-2112-M-007-022-MY3 (H.H.L.).

*chlai@mx.nthu.edu.tw

†hsuihau@phys.nthu.edu.tw

¹S. S. P. Parkin, N. More, and K. P. Roche, *Phys. Rev. Lett.* **64**, 2304 (1990).

²Y. Yafet, *J. Appl. Phys.* **61**, 4058 (1987).

³J. C. Slonczewski, *Phys. Rev. Lett.* **67**, 3172 (1991).

⁴C. H. Lai and K. H. Lu, *J. Appl. Phys.* **93**, 8412 (2003).

⁵M. S. Lin, C. H. Lai, Y. Y. Liao, Z. H. Wu, S. H. Haung, and R. F. Jiang, *J. Appl. Phys.* **99**, 08T106 (2006).

⁶M. S. Lin and C. H. Lai, *J. Appl. Phys.* **101**, 09D121 (2007).

⁷S. Rinaldi and L. Pareti, *J. Appl. Phys.* **50**, 7719 (1979).

⁸A. Sarkis and E. Callen, *Phys. Rev. B* **26**, 3870 (1982).

⁹M. D. Stiles, *Phys. Rev. B* **48**, 7238 (1993); *J. Magn. Magn. Mater.* **200**, 322 (1999).

¹⁰P. Bruno, *Phys. Rev. B* **52**, 411 (1995); *J. Phys.: Condens. Matter* **11**, 9403 (1999).

¹¹W. Baltensperger and J. S. Helman, *Appl. Phys. Lett.* **57**, 2954 (1990).

¹²O. Hellwig, A. Berger, J. B. Kortright, and E. E. Fullerton, *J. Magn. Magn. Mater.* **319**, 13 (2007).

¹³J. Moritz, F. Gracia, J. C. Toussaint, B. Dieny, and J. P. Nozières, *Europhys. Lett.* **65**, 123 (2004).

¹⁴Y. Z. Wu, C. Won, A. Scholl, A. Doran, H. W. Zhao, X. F. Jin,

and Z. Q. Qiu, *Phys. Rev. Lett.* **93**, 117205 (2004).

¹⁵S. Mangin, T. Hauet, P. Fischer, D. H. Kim, J. B. Kortright, K. Chesnel, E. Arenholz, and E. E. Fullerton, *Phys. Rev. B* **78**, 024424 (2008).

¹⁶E. P. Wohlfarth, *J. Phys. F: Met. Phys.* **9**, L123 (1979).

¹⁷P. Hansen, C. Clausen, G. Much, M. Rosenkranz, and K. Witter, *J. Appl. Phys.* **66**, 756 (1989).

¹⁸J. Stöhr, *J. Magn. Magn. Mater.* **200**, 470 (1999).

¹⁹C. T. Chen, Y. U. Idzerda, H. J. Lin, N. V. Smith, G. Meigs, E. Chaban, G. H. Ho, E. Pellegrin, and F. Sette, *Phys. Rev. Lett.* **75**, 152 (1995).

²⁰C. C. Lin, C. H. Lai, D. H. Wei, Y. J. Hsu, and H. P. D. Shieh, *J. Appl. Phys.* **95**, 6846 (2004).

²¹D. H. Wei, Y. J. Hsu, C. C. Lin, C. H. Lai, J. Y. Ou, and J. C. Wu, *J. Magn. Magn. Mater.* **282**, 49 (2004).

²²C. Bordel, S. Pizzini, J. Vogel, K. Mackay, J. Voiron, R. M. Galéra, A. Fontaine, P. Auric, J. B. Goedkoop, and N. B. Brookes, *Phys. Rev. B* **56**, 8149 (1997).

²³M. Bauer, R. Semerad, and H. Kinder, *IEEE Trans. Appl. Supercond.* **9**, 1502 (1999).

²⁴Z. H. Xie, M. Hoffman, P. Munroe, R. Singh, A. Bendavid, and P. J. Martin, *J. Mater. Res.* **22**, 2312 (2007).